Signatures of large peak current lightning strokes during an unusually intense sprite-producing thunderstorm in southern England

Andrea Pizzuti, Jonathan M Wilkinson, Serge Soula, Janusz Mlynarczyk, Ivana Kolmašová, Ondřej Santolík, Robert Scovell, Alec Bennett, Martin Füllekrug

Atmospheric Research 249 (2021) 105357

Contents lists available at ScienceDirect

Atmospheric Research

journal homepage: www.elsevier.com/locate/atmosres

Signatures of large peak current lightning strokes during an unusually intense sprite-producing thunderstorm in southern England

Andrea Pizzuti [a,b,*], Jonathan M. Wilkinson [c], Serge Soula [d], Janusz Mlynarczyk [e], Ivana Kolmašová [f,g], Ondřej Santolík [f,g], Robert Scovell [c], Alec Bennett [a,b], Martin Füllekrug [a]

[a] Department of Electronic and Electrical Engineering, University of Bath, Bath, UK
[b] Bristol Industrial and Research Associates Limited (Biral), Portishead, UK
[c] Met Office, Exeter, UK
[d] Laboratoire d'Aérologie, Université de Toulouse, CNRS, OMP, UPS, Toulouse, France
[e] Department of Electronics, AGH University of Science and Technology, Krakow, Poland
[f] Institute of Atmospheric Physics, The Czech Academy of Sciences, Prague, Czechia
[g] Faculty of Mathematics and Physics, Charles University, Prague, Czechia

ARTICLE INFO

Keywords:
Lightning
Thunderstorm
Natural hazards
TLEs
Sprites
Elves
Halos
EMP
Superbolts

ABSTRACT

During the night of 26–27 May 2017, a mesoscale convective system (MCS) rapidly developed over Cornwall and Devon in the South West of England, producing about 3500 lightning flashes in 3 h and 23 sprites. The MCS-type storm was characterised by a circular shape with a size of about 52,000 km^2 (cloud top temperature lower than -40 °C) and a local minimum in the CG flash rate (~15 min^{-1}), when most of the sprites were observed. The mean intensity of the sprite parent CG strokes was exceptionally high in this case (+170 kA), while the associated charge moment changes ranged from 600 to 2000C km. Two identical detectors, located at different sites in southern England, measured the quasi-static displacement currents induced on metallic electrodes when exposed to the changing atmospheric electric field produced by the storm's discharges. A series of coincident large amplitude short-peak transients, some of which associated with the sprite-producing strokes, were recorded on these detectors. A multi-instrumental analysis of the lightning events producing transient current "spikes" on the electrodes revealed a significant bias towards large peak currents exceeding 100 kA, but only a minor dependence on the impulse charge moment change (iCMC) for those associated with the sprites. We suggest that the current spikes may be induced by a coupling with the electromagnetic impulse radiated by intense lightning discharges. The ease in discriminating such signatures makes the method suitable for monitoring the occurrence of powerful lightning, potentially associated with night-time transient luminous events (TLEs), thereby avoiding the limitations inherent to optical observations and radio noise affecting other receivers.

1. Introduction

The monitoring of lightning discharges is fundamental for nowcasting severe weather and related increased risks for aviation, infrastructures and outdoor activities. Despite the generally low flash density experienced, maritime areas of the UK and northern Europe are a hotspot for intense cloud-to-ground (CG) strokes exhibiting typically large peak current values and a significant amount of energy per stroke, as recently reported by Holzworth et al. (2019). Powerful CG strokes of both polarities may also occasionally result in short-lived (~1 ms to tens of ms) optical phenomena above thunderstorms in the region between the stratosphere and the lower ionosphere that are collectively referred to as transient luminous events (TLEs) (Neubert et al., 2008; Siingh et al., 2012). The most commonly observed types of TLEs are sprites, halos and elves. The sprites are predominantly associated with positive polarity CG strokes occurring in the stratiform region of a mesoscale convective system (MCS). The widely accepted underlying mechanism for sprite production is the streamers development in response to the transient electric field generated at mesospheric altitudes (Pasko et al., 1997), after a large charge moment change (CMC) CG stroke (typically 200–1500C km), once it exceeds the dielectric breakdown threshold (Hu et al., 2002; Lu et al., 2018). Sprites appear as individual or multiple columniform and/or carrot-like structures, which extend vertically from about 40 to 80 km altitude and over a horizontal distance of up to 50 km

* Corresponding author at: Department of Electronic and Electrical Engineering, University of Bath, 2 East, BA2 7AY, Bath, UK.
E-mail address: ap2423@bath.ac.uk (A. Pizzuti).

https://doi.org/10.1016/j.atmosres.2020.105357
Received 6 July 2020; Received in revised form 12 August 2020; Accepted 7 November 2020
Available online 9 November 2020

(Bór, 2013). The quasi-electrostatic heating process leading to sprites is also responsible of a diffuse optical emission region (lasting ~1 ms) at approximately 70–85 km altitude and up to 100 km wide, known as a halo (Barrington-Leigh et al., 2001; Wescott, 2001). Halos may occur alone or preceding a fully structured sprite. Elves are fast (<1 ms), ring-shaped optical emissions that occur higher than halos in the lower ionosphere at 85–95 km altitude, extending around 400–500 km in diameter (Barrington-Leigh and Inan, 1999; Fukunishi et al., 1996). They are produced by heating of the ionosphere by the lightning electromagnetic pulse (EMP) following large peak current (I_{pk} > 80 kA) CG strokes of both negative and positive polarities (Inan et al., 1997; Blaes et al., 2016).

The occurrence of TLEs in Northern Europe and the British Isles is a relatively rare phenomenon if compared to the rest of Europe (Arnone et al., 2020). Even so, serendipitous TLE detections are made available by a network of British amateur astronomers, dedicated primarily to meteor observations. In this paper, we present the case of an exceptional MCS type storm that rapidly developed over Cornwall, in the South West peninsula of England, and produced 23 sprites on the night of 26th/27th May 2017. The storm was widely reported by the British media because of the large number of flashes and several properties struck by lightning (Source: BBC News. South West storms cause property damage, 27 May 2017. URL: https://www.bbc.co.uk/news/uk-england-40069339 [Online; accessed October 27, 2019]). Firstly, we examine the synoptic situation and the storm structure by combining satellite infrared cloud coverage data and radar reflectivity, concurrently with a complete characterization of lightning and sprite activity. Hence, we describe the displacement current measurements obtained by two Biral Thunderstorm Detectors (hereafter BTD) located at a relative distance of about 100 km and based on the technique proposed by Bennett (2013). These sensors operate at frequencies between 1 and 47 Hz and produce signals proportional to the temporal fluctuation of the atmospheric electric field. We focus on the time interval between 0000 UTC and 0140 UTC, when a number of sprites were concurrently captured and the storm was still far enough from the sensors (150 km and 230 km, respectively) to remove the influence of strongly charged overhead cumulonimbus and nearby lightning strokes (≤80 km). Bennett and Harrison (2013) previously described recurrent unusual signals recorded on two prototype BTDs and reported a slight bias towards coincident causative flashes being generally positive and having greater peak current than non-coincident ones. Füllekrug et al. (2013) presented the first example of an unusual quasi-static current signature recorded on a BTD and associated with a sprite-producing stroke, occurred 1000 km away from the sensor. We combine optical and broadband electromagnetic measurements to identify the properties of lightning sources causative of similar current transients, including both the events associated with the observed sprites and the other strong discharges occurred in the same thunderstorm. The results presented confirm that the transient current spikes, coincident on multiple BTDs, are well correlated with bursts of electromagnetic energy, primarily related to distant lightning return strokes (RS) exhibiting peak currents larger than about 100 kA. On the other hand, the spike magnitude is found to be not directly related to the total amount of charge transferred, often lower than the threshold expected for sprite/halo initiation, thus not fully supporting the electrostatic effect caused by halos previously proposed by Bennett and Harrison (2013) and Bennett (2014).

2. Material and methods

2.1. Storm characteristics

The cloud-top temperatures (CTT) are provided by the Meteosat satellite from European Organization for the Exploitation of Meteorological Satellites (EUMETSAT) based on radiometer data in the thermal infrared band (IR) at 10.5–12.5 μm. The temperature accuracy is generally better than 1 K. The parallax error (~15 km for a cloud top at 12 km) is considered for the plots which associate the locations of CG flashes with their parent clouds. The CTT values < -40 °C and < -60 °C are used to define the cloud system outer boundary and the most convective regions, respectively.

Radar reflectivity data from the UK Met Office weather radar network are used to describe the storm structure and its precipitation pattern evolution with a temporal resolution of 5 min. The Met Office 3D radar composite is compiled from a network of 15 operational C-band radars. The spatial resolution is 1 km horizontally and 500 m vertically, extending to an altitude of about 12 km (Scovell and Al-Sakka, 2016). Radar maps reported in this article displays the vertical column-maximum reflectivity at each horizontal grid point (central panel), the maximum reflectivity along a line at a constant altitude and constant northing, going west to east (side panel), and the maximum reflectivity along a line at a constant altitude and constant easting, going north to south (top panel). The map domain size is 250 km in easting 350 km in northing.

2.2. Lightning activity data

The data used for the analysis of the overall lightning activity related to the storm is supplied by Météorage, a French company providing a lightning location system (LLS) with high performance over the area of interest. The network detects the Low Frequency (LF) radiation emitted by lightning return strokes and combines magnetic direction finding (MDF) and time-of-arrival (TOA) techniques to deliver accurate information such as location, timing, polarity and peak current. The detection efficiency of the network for CG flashes containing at least one stroke with a peak current greater than 2 kA is typically greater than 95% and the median location accuracy is around 100 m (Schulz et al., 2016). Peak current estimates are validated with a median absolute accuracy of the order of 15–20% for negative CG subsequent RS (Schulz et al., 2016). Some uncertainty remains about the intensity estimates of first negative RS, positive RS and intra-cloud IC discharges, as no direct validation is currently available.

Additional data from the World Wide Lightning Location Network (WWLLN) are also used to complete the identification of CG strokes that produced the sprites. WWLLN is based on a worldwide network of VLF receivers which continuously detect lightning sferics, providing real-time information on global lightning activity and time, location and intensity data for each stroke detected. The detection efficiency of WWLLN for CG strokes of about 30 kA is estimated in approximately 30% globally (Hutchins et al., 2012).

2.3. Displacement current technique

The quasi-static current measurements were performed using the BTD-300 instrument, designed to monitor total lightning activity within a range of about 80 km (Bennett, 2017). The detector uses 3 co-located stainless-steel passive antennas of approximately 0.1 m^2 each, whose geometry has been modelled to enhance the effect of the vertical electric field from lightning, causing a change in the surface charge distribution on the electrodes, while avoiding corona initiation under the strong electric field below a thundercloud. Each antenna generates a displacement current proportional to the rate of change of electric field surrounding the instrument, which flows from the surface of the conductor to the ground through a high impedance resistor. The three current signals are converted into voltage with low-noise current amplifiers (1 V ~ 45 nA), embedded within the supporting insulators, and digitized at 16-bit resolution. The insulators are heated and shielded for all weather sampling. The total electric field change from a lightning flash is then proportional to the amplifier's integrated voltage output for the flash duration. The signal measured is also suitably filtered in order to achieve an operating bandpass 1–47 Hz, thus removing the DC currents and the 50 Hz mains frequency and rejecting unwanted man-made radio interferences. At these frequencies, the largest percentage of the

current induced on the antenna, within about 80 km from the flash, is mainly due to the net electrostatic field change produced by the lightning flash, proportional to its charge moment and decreasing as the inverse cube of distance.

Two identical BTDs were operating simultaneously at the time of the storm, sampling the induced current values at 100 Hz. One (BTD1) was located in Portishead, UK (51.483 N, 2.769 W) and the other (BTD2) approximately 100 km eastward at Chilbolton Observatory (51.145 N, 1.438 W). The raw data were stored on a local PC and time-stamped in UTC using the PC-time, which was synchronized to a Network Time Protocol (NTP) server. This method introduces a time drift in the data, often exceeding ±100 ms with respect to the GPS-time. Nevertheless, given the low rate incidence of current spikes and the combination with data from other lightning networks, this uncertainty was sufficient to unambiguously identify the flashes associated with the recorded signals.

2.4. Broadband EM measurements

Recordings of VLF waveforms of sprite-parent strokes have been performed at a 3-component receiving station on the summit of La Grande Montagne (43.941 N, 5.484E) in southern France at approximately 1000 km from the storm. The station is equipped with two perpendicular magnetic loop antennas and a spherical electric antenna, to monitor the vertical upward electric field component and horizontal eastward and southward magnetic field components with a 50 kHz sampling rate. The system is set to log 144 s long waveforms every five minutes (Santolík and Kolmašová, 2017). 12 out of the 23 + CG strokes associated with the sprites were thus recorded by the station.

The current moment waveforms (CMW) and the CMC shown in this paper were calculated using the method presented by Mlynarczyk et al. (2015). The analysis is based on the ELF magnetic field data recorded from the Hylaty station in Poland (Kułak et al., 2014), taking into account the impulse response of the receiver and the Earth-ionosphere wave propagation. The iCMC and CMC for a CG lightning stroke are estimated respectively from the peak amplitude of the recorded impulse and by integrating the CMW during the whole variation due to the lightning return stroke and the subsequent continuing current.

2.5. Sprite imaging

The UK Meteor Network (UKMON) is an amateur network of meteor detection cameras that monitor the night sky continually and record any meteor activity visible from the UK since 2012. During the night of the storm, an optical camera system located at Wilcot observing station (51.352 N, 1.801 W; 133 m a.s.l.) was pointing westwards, in the direction of the thunderstorm. The station includes a high-resolution low-light CCD camera with a standard PAL frame rate of 25 fps, corresponding to 40 ms (20 ms deinterlaced) resolution, and equipped with a 4–12 mm F/1.2 lens. The camera was operating in trigger mode by the UFOCaptureHD2 software developed by SonotaCo, which detects any brightness change above a customized threshold to record TLEs.

3. Results and discussion

3.1. Storm and sprites characteristics

The night of 26–27 May 2017 was warm and moist, continuing the warmth produced by ample solar heating of the moist boundary layer earlier in the day. According to data from the Met Office, the temperatures in the middle of the afternoon had ranged from 25 to 30 °C over the South-West peninsula of the UK and these had only cooled to around 18–20 °C by 23 UTC. The European Storm Forecast Experiment (ESTOFEX; see http://www.estofex.org) issued a threat level 1 for the risk of thunderstorms developing rapidly into organized clusters, crossing the W-English Channel and affecting SW-England during nighttime, with possible large hail and excessive rainfall. The Met Office analysis chart at 00 UTC in Fig. 1 shows the trough line associated with the storm of interest that affected Cornwall and Devon.

Thermal infra-red (IR) data from Meteosat satellite suggest that the storm formed over the sea, close to southern coast of Cornwall, with lightning starting around 2330 UTC, when the area of the cloud system with CTT lower than −40 °C (A(−40)) extended over 11,300 km^2 (Fig. 2a). It is possible that the progress of the storm northwards over the steep slopes of relatively high grounds present over the South West peninsula caused the updrafts to grow stronger through orographic enhancement and the storm to intensify. The lightning activity peaked between 0000 UTC and 0200 UTC, before the storm gradually dissipated into Wales. Fig. 2b reveals that the flash rate reached its maximum (~35 fl min^{-1}) at 0110 UTC and stabilized around that value for the next 30 min. The overall peak of CG flash rate was preceded by a minimum, coinciding with local maxima of +CG proportion around 20–30% and a significant increase in the average peak current of the positive CG flashes reaching ~ + 105 kA, as seen in Fig. 2b. The average amplitude of +CG was constantly larger than for -CG strokes, which stayed below an absolute average magnitude of −20 kA throughout the storm. The number of +CG flashes remained almost constant until 0300 UTC, consistent with a positive charge layer reservoir in the stratiform region of the dissipating MCS (Marshall and Rust, 1993; Williams, 1998; Lu et al., 2009).

The 23 sprites were observed in the period 0015–0140 UTC, as summarized in Table 1. Several studies link the sprite occurrence to MCS convective development and indicate that sprites are more likely to be produced during the transition between the mature and the dissipating stage of the MCS, when the -CG flash rate maximizes and the overlying coldest CTT area is close to its maximum extent (São Sabbas and Sentman, 2003; Lang et al., 2016). By contrast, the sprite activity described in this article started relatively early, during the growing stage of the storm, when the cloud size (CTT lower than −40 °C) was of the order of 22,000 km^2 and the coldest CTT region A(−60) was limited to ~1600 km^2. Most of the sprites occurred in the 30-min interval starting at 0030 UTC and appeared distributed in two clusters (Fig. 2b), well synchronized with a convective lull featuring a minimum in the total flash rate before it rapidly recovered later. The sprite-parent positive CG (SP + CG) strokes were predominantly located along the coastline, ahead of the highest flash density areas and adjacent to the frontal convective core (shown in Fig. 3 and Fig. 4). Previous works (Lang et al., 2004; Lu et al., 2009) revealed that most of the +CG strokes exhibiting large CMC (≥ 1500C km), originate from flashes that start in the convective region of a MCS and then extend horizontally over several tens of km during the long continuing current phase (~10 to more than 100 ms), lowering charge mainly from the upper positive charge in the stratiform region. In

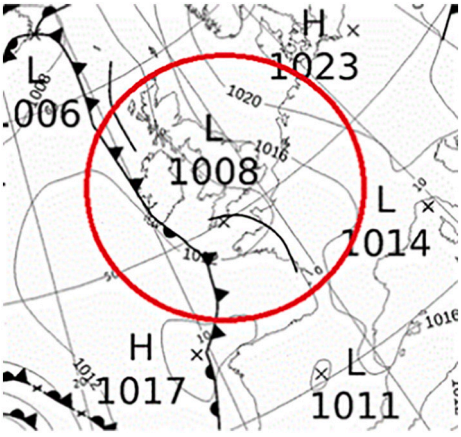

Fig. 1. UK Met Office surface synoptic chart valid at 0000 UTC on the 27 May 2017, showing the trough line associated with the storm in Cornwall. (Credits: Met Office, 2017).

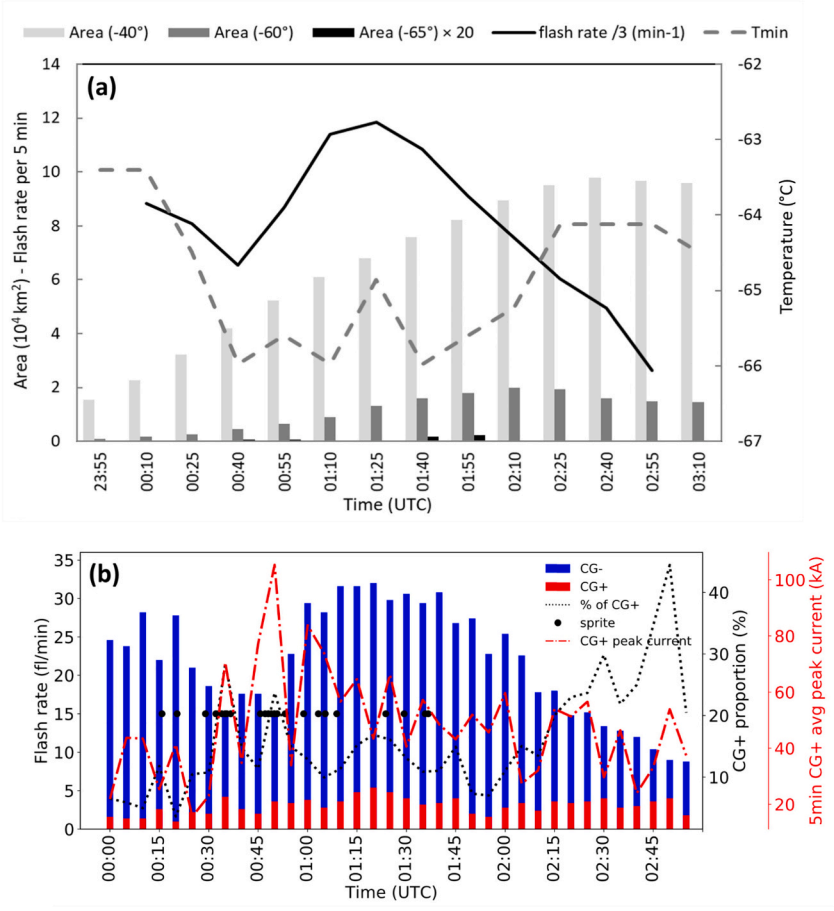

Fig. 2. Analysis of the storm structure and lightning activity, starting from about 15 min before the first sprite occurred. (a): Time series of minimum value of cloud top temperature T_{min} and areas with CTT < -40 °C, <-60 °C and < -65 °C. The scale for areas is 10^4 km^2 and A(−65) values are multiplied by 20. Solid black line shows the flash rate evolution for the same period. (b): CG flash rate by polarity (blue stacked bar for -CG, red stacked bar for +CG), +CG proportion (black dotted line) and 5-min average peak current of +CG (red dashed line). The black circles correspond to the time of observed sprites.

Table 1
Characteristics of the 23 TLE events captured on the 27th May 2017: date, time, location, peak current and iCMC/CMC of the SP + CG stroke; associated sprite morphology.

Time (UTC)	Lat	Lon.	Location	I_{pk} (kA)	iCMC (C km)	CMC (C km)	Sprite type
00:16:32.133	50.5528	−4.4841	Land	72	240	1035	Column
00:21:12.310	50.5522	−4.5973	Land	59	120	700	Column
00:29:56.216	50.631	−4.6589	Land	65	118	1063	Column
00:33:09.220	50.6735	−4.6712	Land	170	440	825	Column
00:34:59.890	50.6174	−4.3797	Land	203	685	847	Column
00:35:59.713	50.695	−4.644	Land	160	237	1117	Column
00:36:32.903	50.688	−4.6769	Land	158	438	610	Column
00:37:43.357	50.7072	−4.6764	Sea	278	558	825	Jellyfish
00:46:57.243	50.8219	−4.5387	Land	115	375	1137	Column
00:48:25.440	50.8169	−4.4895	Land	110	338	1957	Column
00:49:23.343	50.8691	−4.4446	Land	126	359	1103	Column
00:50:17.590	50.8437	−4.7128	Sea	218	637	909	Irregular
00:51:14.609	50.8664	−4.7244	Sea	285	900	977	Jellyfish
00:52:06.834	50.8523	−4.7283	Sea	263	789	1052	Jellyfish
00:54:37.391	50.7554	−4.3555	Land	282	509	1045	Irregular
01:00:17.620	50.8292	−4.4109	Land	156	548	769	Column
01:04:50.625	50.9888	−4.7773	Sea	207	654	877	Jellyfish
01:06:59.369	51.0191	−4.7597	Sea	216	399	1344	Column
01:10:31.743	51.0384	−4.7295	Sea	244	991	1510	Jellyfish
01:25:43.685	50.5879	−4.7949	Land	137	401	881	Column
01:31:23.046	50.7079	−4.8522	Sea	79	261	1104	Column
01:37:53.252	51.0609	−4.5152	Sea	219	662	732	Jellyfish
01:38:50.139	51.0409	−4.2123	Land	182	526	1048	Column

other case studies, sprites were also found to occur over +CGs in convective regions of asymmetric MCS, revealing eventual evidence of anomalous positive charge layers near mid-levels (T ∼ −20 °C) rather than the more common negative charge, as previously observed by Lang et al. (2016). The video sequences show that the sprites were mainly prompt events (i.e. delayed by only few ms with respect to the return stroke), exhibiting column (narrow, straight and mostly uniform elements) or jellyfish features (more elongated, irregular shapes, usually with very visible streamers extending downwards from a bright head) as shown in Fig. 5. We noted that jellyfish/irregular sprite groups occurred

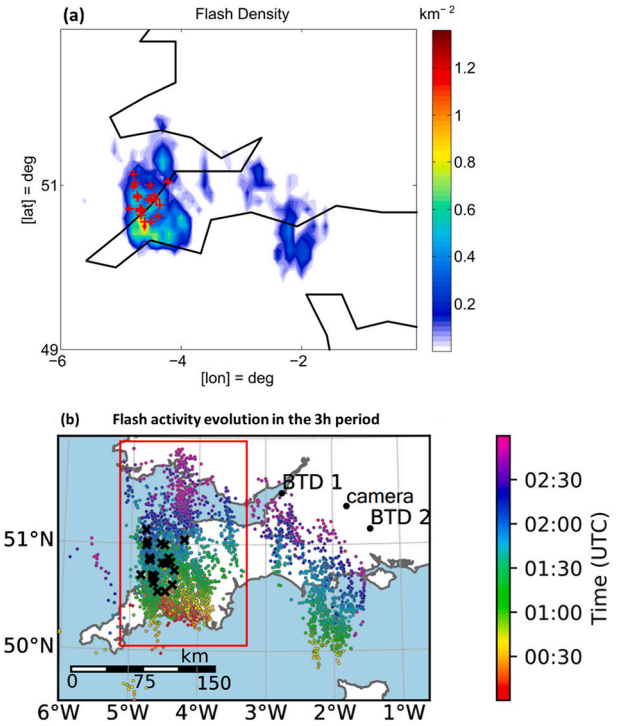

Fig. 3. (a): CG flash density (km^{-2}) averaged over a 0.1° × 0.1° grid during the 3 h after 00 UTC on 27 May 2017; the SP + CG strokes are indicated by red crosses. (b): Flash temporal distribution during the same period, with black crosses indicating the locations of SP + CG.

mostly in the second half of the observation period and the associated +CG were confined on the sea surface, showing larger peak currents and iCMC on average (Table 2). In general, the peak current of the SP + CG strokes ranged between +60 and + 285 kA, with an average of +170 kA, a value significantly larger than the average value of about +60 kA found previously (São Sabbas et al., 2003; Lyons et al., 2003). SP + CG strokes showing similarly large peak currents are found to be associated with very low flash-rate and limited extent winter thunderstorms in the UK (Pizzuti et al., 2020). On the other hand, the estimated CMC values varied between 600 and 2000C km, accordingly with the typical values found for sprite production (Lu et al., 2018).

3.2. BTD measurements

During the continuous operation of BTD1 and BTD2 over the sprite activity period, peculiar transient current pulses were recorded by the sensors. Such signals feature a narrow peak, whose amplitude is up to 3 orders of magnitude larger with respect to the fair-weather current (~10 pA). In this work, we identified the transients that were coincident on both sensors and classified an event as spike, applying a selection criterion that looked at the overall signal shape (i.e. single peak and no recovery curve), the absolute peak amplitude (≥1 nA on at least one of the sensors), the consistency of signal polarity on the primary and secondary antenna of each sensor, quantified by a positive covariance threshold. The events that satisfied the previous criterion represent about 80% of the total 62 CG strokes reported in the domain considered and exceeding +100 kA (median + 167 kA). -CG stroke intensities remained lower, within the −50 kA limit in the storm area over Cornwall. The large amplitude transients are clearly visible and well correlated, despite the relative distance of about 100 km between the two sensors (Fig. 6). The relatively short durations are uncharacteristic of

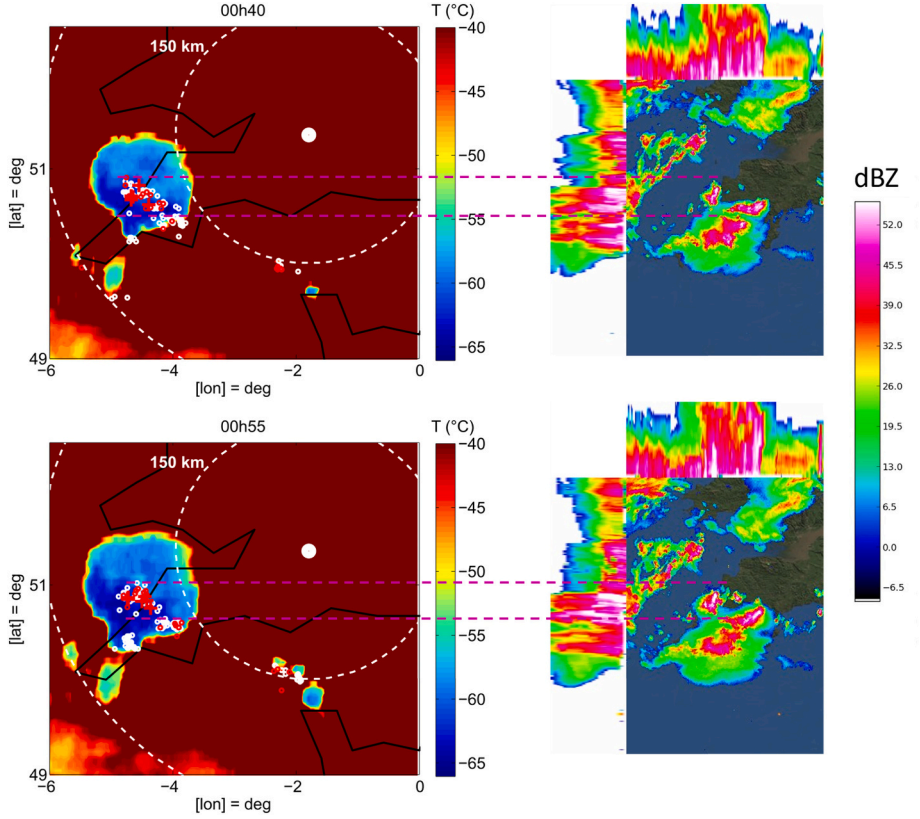

Fig. 4. Meteosat cloud top temperature (CTT) maps (left) and corresponding Met Office radar reflectivity (dBZ) (right) at the time 0040 and 0055 UTC. The locations of negative and positive CG flashes over the 5 min around the time of satellite scan are reported (white and red circles). The SP + CG strokes are indicated by the red crosses. Dashed circles indicate the reference distance from the camera.

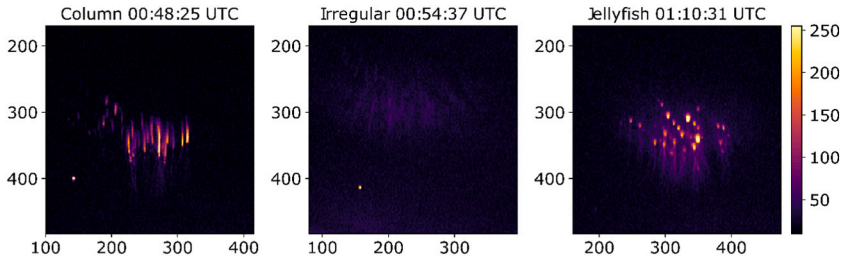

Fig. 5. Different morphology sprites captured from Wilcot (UK). The peak brightness field is obtained by de-interlacing the original video sequence. (Credits: UKMON).

Table 2
Properties of the SP + CG by observed sprite morphologies: average peak current and iCMC/CMC; land/sea contrast; associated BTD spikes percentage.

	Column	Jellyfish/irregular
Total events	15	8
I_{pk} (kA)	134	250
iCMC (C km)	365	722
CMC (C km)	1036	981
land/sea ratio	86% on land	87.5% on sea
BTD spike ratio	46%	100%

BTD recorded currents from lightning at closer distance from the sensor, in the range of 10–80 km, which are seen to last typically ~200–500 ms due to the combined effect of pre-discharge processes, intra-cloud (IC) charge neutralization and multiple return strokes as shown in Fig. 7. By contrast, typical spike signals show no evidence of recovery curve, a polarity often reversed with respect to the causative stroke and a higher peak frequency (~40 Hz). Evidence of the BTD spike polarity reversal was previously noted by Bennett and Harrison (2013).

16 out of the 23 SP + CG strokes induced similar signatures on the BTDs, but no discernible differences in shape were found with respect to non-TLE spikes (Fig. 6 and Fig. 7). However, the subset of TLE-associated events revealed a significantly higher proportion of spikes linked to the more impulsive SP + CG that triggered jellyfish/irregular sprites (as shown in Table 2). It must be pointed out that most of the sprites occurred promptly after the return stroke, so it was not possible to separate the contribution of the return stroke itself from the eventual subsequent combined effect of continuing current and current flowing in the sprite body. This limitation is imposed by the 100 Hz sampling rate utilized by the BTD, that may lead in some cases to under sample the recorded spike signals, thus potentially masking additional current features.

Broader and more complex BTD signals associated with flashes beyond 100 km are better explained by strokes exhibiting longer continuing current (> 20 ms) and producing delayed sprites. These signals have typically lower amplitudes (i.e. generally not exceeding ~0.3–0.5 nA) compared to the shorter-duration BTD spikes. A very peculiar signal shape was recorded in the unique case of the sprite at 00:48:25 UTC, produced by a + 108 kA SP + CG stroke. The sprite was characterised by two groups of columns, the second of which shows a peak in the luminosity about 20 ms after the return stroke (shown in Fig. 5), in coincidence of a clear resurgence of the ELF current moment waveform (Fig. 8b). The corresponding BTD output shows two separate subsequent peaks on both the sensors. We cannot exclude that the second peak is associated with the delayed brighter sprite group, given the flash had a multiplicity 1 and no other strokes were reported in the following 300 ms. This event suggests that currents flowing in the body of delayed sprites may eventually alter the overall signal shape, resulting in the onset of a double peak pattern, although showing significantly lower amplitudes with respect to prompt events.

3.2.1. *Relation between BTD current spikes and lightning properties*

In order to investigate the existing link between the observed BTD signals selected as spikes and the properties of causative lightning, we examined independent measurements of the coincident RS and estimated parameters as the peak current provided by Meteorage and the CMC, reconstructed from the Hylaty ELF magnetic field measurement of RS pulses.

In Fig. 9a, the measured BTD spike peak amplitudes are plotted versus the estimated total CMC of related CG strokes. The CMC values refer to both 16 SP + CG strokes and other strong +CG strokes for which ELF measurements were available but no TLE was reported by the observers. Data do not show any apparent difference between the two cases, with a wide range of possible CMC values for a given peak amplitude. On the other hand, a focus on the sprite-associated sprites shows the spike absolute magnitude to slightly increase linearly with the iCMC and the peak current of the causative RS pulse, as seen in Fig. 9b

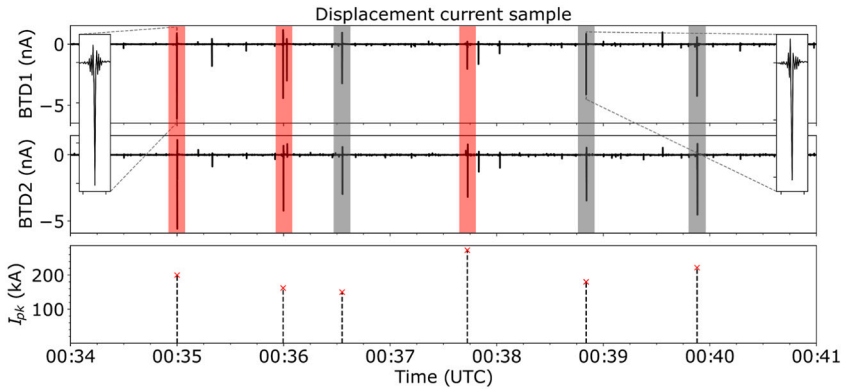

Fig. 6. Displacement current output of the primary antenna on BTD1 (Portishead, UK) and BTD2 (Chilbolton, UK) between 0034 and 0041 UTC. The large amplitude current spikes shown are well correlated over the distance on the two detectors. Red and grey areas highlighted in the plot indicates the spikes featuring similar characteristics, related to the SP + CG and other strong +CG without TLEs, respectively.

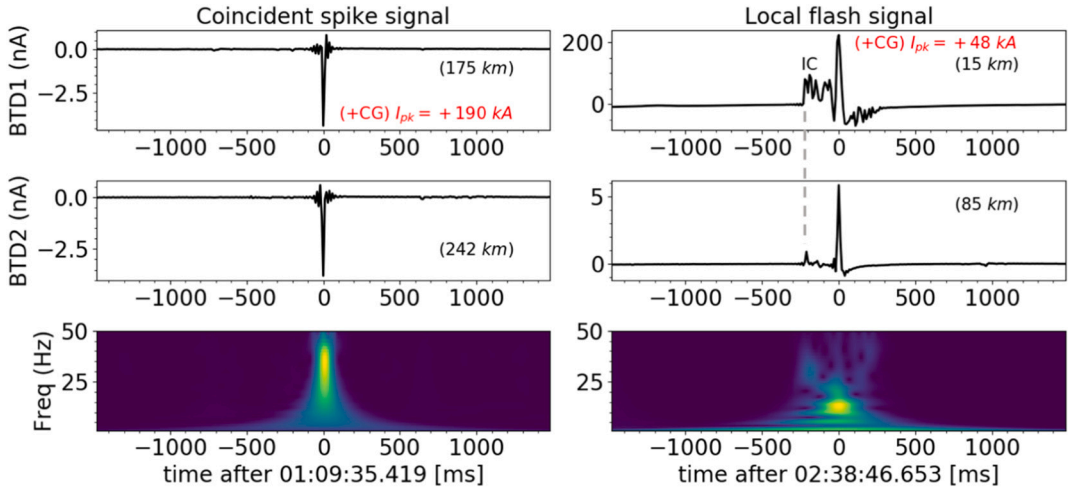

Fig. 7. Comparison between a coincident current spike (left) induced by a distant +190 kA CG return stroke and a local flash (right) recorded at closer range when a secondary storm cell approached to the sensors. The second case shows the peak amplitude associated with a + 48 kA CG distant 18 km from BTD1, preceded ~200 ms before by an IC pulse and followed by the recovery curve. In this example, the current spike polarity is reversed with respect to the causative discharge. Relative distances between each sensor and the source are indicated in brackets.

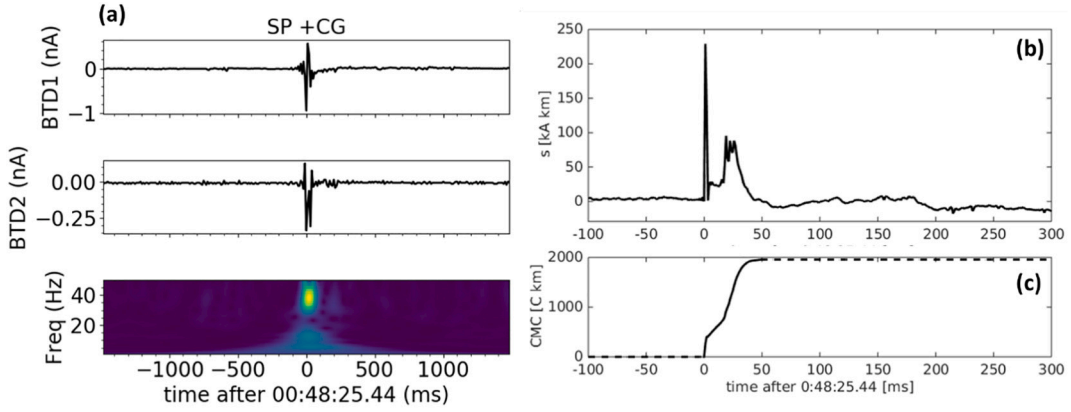

Fig. 8. Peculiar double peak signature of the SP + CG at 00:48:25 UT on the two BTD detectors (a). The associated CMW (b) and CMC (c) were obtained from the ELF recordings in Poland. The CMW shows the hump in the continuing current coincident with the peak luminosity of the delayed sprite column group, about 20 ms after the parent stroke, and correlated with the second peak feature on the BTD displacement current sample.

and c. The emergence of similar current transients was previously attributed by Bennett and Harrison (2013) and Bennett (2014) to the electrostatic effect of a horizontal mesospheric charge sheet distribution related with a halo, extending the range of detection of such signatures with respect to typical flashes and accounting for a signal polarity reversal depending on the distance from the detector (Sonnenfeld and Hager, 2013). However, such explanation requires the occurrence of CG strokes moving large amount of charge, responsible of the quasi-electrostatic (QES) heating at mesospheric altitudes associated with halos. For the positive and negative causative strokes, the median iCMC associated with halo production are +474 and − 461C km, respectively, i.e. larger than those associated with sprite production (+200 and − 300C km, respectively) (Lu et al., 2013; Lu et al., 2018), with a small percentage of halo/sprites found to initiate below these thresholds. In addition, simulations reported by Pérez-Invernón et al. (2016) have shown that lightning-driven charge enhancements in the lower ionosphere, associated with halos, are not consistent with an increase in the electrostatic field at ground level at distances further than 100 km from the source. The result found does not allow an unambiguous association with sprite halos, but suggests that the occurrence of strong discharges, characterised by an incidental combination of large peak current and high impulsive charge moment and associated with this class of TLEs (Soula et al., 2020), may eventually lead to the observed spikes as observed during the storm in Cornwall. By contrast, the BTD spikes have been regularly recorded in association with elves, thus strengthening the bond with intense RS pulses and the subsequent EMP (Pizzuti et al., 2019a, 2019b).

As a further step, we inspected the 3-components VLF waveforms recorded in Rustrel (France). The station recorded 12 RS pulses among the 23 sprite events, due to the system recording configuration. The azimuths of arrival on incoming radiation were estimated using the 3-component analysis and confirm that all 12 recorded strong signals arrived from the direction which corresponds to locations of causative strokes with and average error of only 1.3°. The area where the sprites occurred was well localized and far from the receiving station (~ 1000 km), thus the distance and angle of arrival was very similar for the 12 events. For each RS, the estimated ground wave peak amplitude is plotted as a function of the peak current provided by Météorage and the corresponding BTD signal peak, showing their proportionality (shown in Fig. 10, upper panel). We therefore obtained an independent verification of the BTD spike magnitude relationship with the RS peak current amplitude (lower panel).

In order to evaluate the propagation attenuation of the BTD recorded signals, we combined the data from the two sensors used. The relative

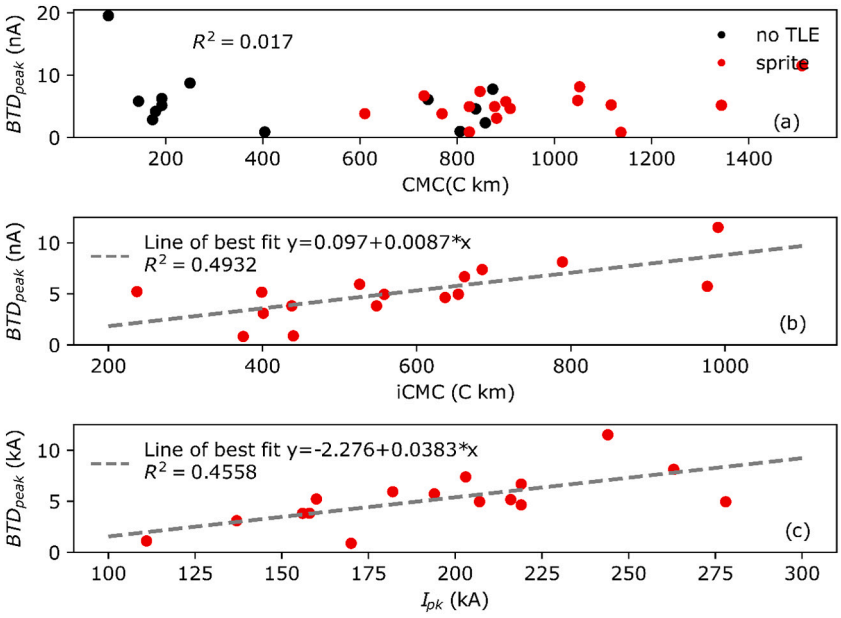

Fig. 9. (a) Independent ELF measurements of lightning return strokes associated with coincident BTD current spikes show a wide range of possible CMC values, often below the threshold for sprite/halo initiation, and suggest that their peak amplitudes do not depend on the total amount of charge transferred. On the other hand, the probability of detecting a similar signature associated with a sprite-producing stroke increases for larger impulse charge moment changes (iCMC) (b) and peak currents (c).

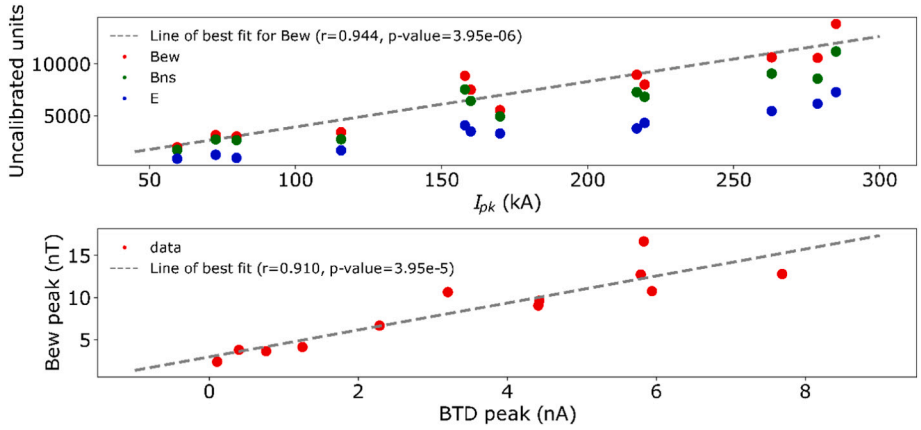

Fig. 10. The 3-component VLF station in Rustrel (France) recorded 12 of the sprite-producing return strokes during the storm in Cornwall. Related ground wave peak amplitudes are plotted as a function of the peak current estimates provided by Météorage (upper panel). A comparison with the BTD spike magnitudes provides an independent verification of the relation between spike occurrence and RS peak current (lower panel).

distance between each sensor and the lightning sources was determined using the CG stroke location reported by Météorage. In Fig. 11, we plotted the ratio between BTD spike amplitude and related peak current of causative stroke versus the distance from the source. With this data set, we performed a nonlinear fit assuming the relation between the BTD_{peak} (nA) and the propagating distance from the source D (km) to have the form of $BTD_{peak}/I_{pk} = a \cdot D^{-b}$, where a and b are a constant and the attenuation rate, respectively. Applying the least squares fitting method to the unaveraged data, the BTD signal amplitude is found to decrease with the distance from the source as $D^{-0.86}$. A similar model form was previously used by Chang et al. (2014) to describe the attenuation rate of ULF/VLF lightning sferics, propagating in the earth-ionosphere cavity.

4. Summary and conclusions

We presented the first multi-instrumental analysis of a rare thunderstorm system producing 23 sprites in the UK. The majority of observed sprites occurred prior to the transition between mature and dissipating stage of the MCS and coincided with a convective lull, characterised by a minimum in the flash rate (~15 fl min^{-1}) and a peak of 30% in the fraction of +CG return strokes. The peak currents of detected SP + CG reached an unusually large average of +170 kA, while the overall intensity of +CG RS was 51.6 kA on average. Evidence of a land/sea contrast between the SP + CG triggering column and jellyfish/irregular sprites was found, the latter being confined on the sea surface and generally characterised by larger peak current (+250 kA) and iCMC (722C km).

Concurrent displacement current measurements performed at two different sites, distant 150 and 230 km from the storm, revealed coincident current spikes associated with intense CG RS and differing significantly from typical flash shapes observed at closer range. Independent recordings of ELF/VLF lightning waveforms showed that the spike emergence is not correlated to the total CMC of the causative stroke but suggest a close dependence on the RS peak current intensity and the radiated electromagnetic impulse. In addition, a significantly higher proportion of the TLE-related spikes is found associated with jellyfish/irregular events and thus to the more impulsive SP + CG strokes.

The reported nanoampere scale signatures observed using the unique technique exploited by the BTD sensors, immune to most of man-made radio interference, can potentially provide a complementary method

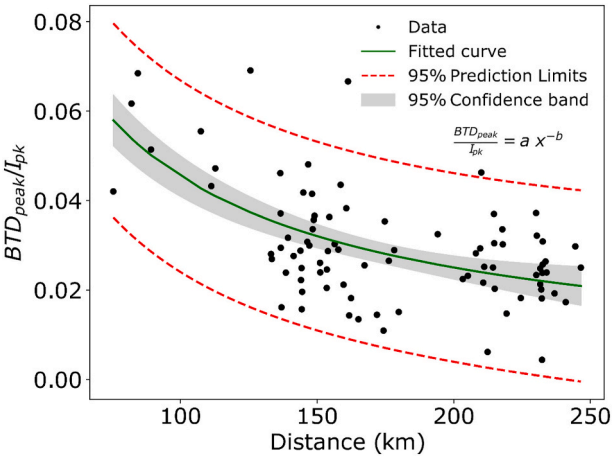

Fig. 11. Attenuation of BTD current spike peak amplitude, divided by the peak current of causative stroke, on the distance from detector. The nonlinear least squares fit applied to the unaveraged data and assuming a power law model curve is shown and suggest a dependence on $D^{-0.86}$, where D is the distance from the source in km.

for monitoring the regional ($\leq$ 1000 km) occurrence of powerful remote lightning and locate them by using the integrated Low Frequency (LF) direction finder. The present data indicates that the detection efficiency for distant strokes ($>$ 100 km) exceeding 100 kA is about 80%, as estimated using Météorage lightning data as reference for this specific case. For larger peak currents, this value rises significantly to 100% (i.e. all reported CG strokes above 200 kA in the case analysed corresponded to coincident signal on the BTD sensors). The observed transient signals are easily discernible above the fair-weather current level and their seasonal variability (Bennett and Harrison, 2013), showing a predominance of this type of events during the winter season (November to March) on sea/coastal areas of northern Europe as the English Channel, is consistent with the distribution of superbolt lightning (Holzworth et al., 2019). This study then could likely contribute to better characterize small-scale winter thunderstorms with very low flash rates in northern Europe and evaluate related risks for maritime operations and aviation. Furthermore, the association between large peak currents and intense EMP also suggests that the method can be profitably used for TLE research, especially as a proxy of night-time EMP producing elves (Pizzuti et al., 2019a, 2019b), avoiding the limitations imposed by optical observations and the occasional rejection of related strokes by the processing algorithms of VLF/LF lightning detection systems.

Declaration of Competing Interest

None.

Acknowledgments

The authors thank the helpful comments of two anonymous reviewers that have led to improve this manuscript. They are also grateful to the UKMON and Richard Kacerek for providing the sprite video sequences. They would like to thank Stephane Pedeboy (Météorage) and Bob Holzworth (WWLLN) for providing the lightning data for this study. The work of AP is supported by the European Union's Horizon 2020 research and innovation programme under the Marie Sklodowska-Curie grant agreement 722337. The work of IK and OS was supported by European Regional Development Fund-Project CRREAT (CZ.02.1.01/0.0/0.0/15_003/0000481), by the GACR grant 20-09671S, and by the Praemium Academiae award of the Czech Academy of Sciences.

References

Arnone, E., Bór, J., Chanrion, O., Barta, V., Dietrich, S., Enell, C.F., Farges, T., Füllekrug, M., Kero, A., Labanti, R., Mäkelä, A., 2020. Climatology of transient luminous events and lightning observed above Europe and the Mediterranean Sea. Surv. Geophys. 41 (2), 167–199.
Barrington-Leigh, C.P., Inan, U.S., 1999. Elves triggered by positive and negative lightning discharges. Geophys. Res. Lett. 26 (6), 683–686.
Barrington-Leigh, C.P., Inan, U.S., Stanley, M., 2001. Identification of sprites and elves with intensified video and broadband array photometry. J. Geophys. Res. Space Physics 106 (A2), 1741–1750.
Bennett, A.J., 2013. Identification and ranging of lightning flashes using co-located antennas of different geometry. Measurement Science and Technology 24 (12), 125801.
Bennett, A.J., 2014. Modification of lightning quasi-electrostatic signal by mesospheric halo generation. J. Atmos. Sol. Terr. Phys. 113, 39–43.
Bennett, A.J., 2017. Electrostatic thunderstorm detection. Weather 72 (2), 51–54.
Bennett, A.J., Harrison, R.G., 2013. Lightning-induced extensive charge sheets provide long range electrostatic thunderstorm detection. Physical Review Letters 111 (4), 045003.
Blaes, P.R., Marshall, R.A., Inan, U.S., 2016. Global occurrence rate of elves and ionospheric heating due to cloud-to-ground lightning. J. Geophys. Res. Space Physics 121 (1), 699–712.
Bór, J., 2013. Optically perceptible characteristics of sprites observed in Central Europe in 2007–2009. J. Atmos. Sol. Terr. Phys. 92, 151–177.
Chang, S.C., Hsu, R.R., Huang, S.M., Su, H.T., Kuo, C.L., Chou, J.K., Lee, L.J., Wu, Y.J., Chen, A.B., 2014. Characteristics of TLE-producing lightning in a coastal thunderstorm. J. Geophys. Res. Space Physics 119 (11), 9303–9320.
Fukunishi, H., Takahashi, Y., Kubota, M., Sakanoi, K., Inan, U.S., Lyons, W.A., 1996. Elves: Lightning-induced transient luminous events in the lower ionosphere. Geophys. Res. Lett. 23 (16), 2157–2160.
Füllekrug, M., Kolmasova, I., Santolik, O., Farges, T., Bór, J., Bennett, A., Parrot, M., Rison, W., Zanotti, F., Arnone, E., Mezentsev, A., 2013. Electron acceleration above thunderclouds. Environmental Research Letters 8 (3), 035027.
Holzworth, R.H., McCarthy, M.P., Brundell, J.B., Jacobson, A.R., Rodger, C.J., 2019. Global distribution of superbolts. Journal of Geophysical Research: Atmospheres 124 (17–18), 9996–10005.
Hu, W., Cummer, S.A., Lyons, W.A., Nelson, T.E., 2002. Lightning charge moment changes for the initiation of sprites. Geophys. Res. Lett. 29 (8), 120–121.
Hutchins, M.L., Holzworth, R.H., Brundell, J.B., Rodger, C.J., 2012. Relative detection efficiency of the world wide lightning location network. Radio Sci. 47 (06), 1–9.
Inan, U.S., Barrington-Leigh, C., Hansen, S., Glukhov, V.S., Bell, T.F., Rairden, R., 1997. Rapid lateral expansion of optical luminosity in lightning-induced ionospheric flashes referred to as 'elves. Geophys. Res. Lett. 24 (5), 583–586.
Kułak, A., Kubisz, J., Kłucjasz, S., Michalec, A., Młynarczyk, J., Nieckarz, Z., Ostrowski, M., Zięba, S., 2014. Extremely low frequency electromagnetic field measurements at the Hylaty station and methodology of signal analysis. Radio Sci. 49 (6).
Lang, T.J., Rutledge, S.A., Wiens, K.C., 2004. Origins of positive cloud-to-ground lightning flashes in the stratiform region of a mesoscale convective system. Geophys. Res. Lett. 31 (10).
Lang, T.J., Lyons, W.A., Cummer, S.A., Fuchs, B.R., Dolan, B., Rutledge, S.A., Krehbiel, P., Rison, W., Stanley, M., Ashcraft, T., 2016. Observations of two sprite-producing storms in Colorado. Journal of Geophysical Research: Atmospheres 121 (16), 9675–9695.
Lu, G., Cummer, S.A., Li, J., Han, F., Blakeslee, R.J., Christian, H.J., 2009. Charge transfer and in-cloud structure of large-charge-moment positive lightning strokes in a mesoscale convective system. Geophys. Res. Lett. 36 (15).
Lu, G., Cummer, S.A., Li, J., Zigoneanu, L., Lyons, W.A., Stanley, M.A., Rison, W., Krehbiel, P.R., Edens, H.E., Thomas, R.J., Beasley, W.H., 2013. Coordinated observations of sprites and in-cloud lightning flash structure. Journal of Geophysical Research: Atmospheres 118 (12), 6607–6632.
Lu, G., Yu, B., Cummer, S.A., Peng, K.M., Chen, A.B., Lyu, F., Xue, X., Liu, F., Hsu, R.R., Su, H.T., 2018. On the causative strokes of halos observed by isual in the vicinity of North America. Geophys. Res. Lett. 45 (19), 10–781.
Lyons, W.A., Nelson, T.E., Williams, E.R., Cummer, S.A., Stanley, M.A., 2003. Characteristics of sprite-producing positive cloud-to-ground lightning during the 19 July 2000 STEPS mesoscale convective systems. Mon. Weather Rev. 131 (10), 2417–2427.
Marshall, T.C., Rust, W.D., 1993. Two types of vertical electrical structures in stratiform precipitation regions of mesoscale convective systems. Bull. Am. Meteorol. Soc. 74 (11), 2159–2170.
Młynarczyk, J., Bór, J., Kulak, A., Popek, M., Kubisz, J., 2015. An unusual sequence of sprites followed by a secondary TLE: an analysis of ELF radio measurements and optical observations. J. Geophys. Res. Space Physics 120 (3), 2241–2254.
Neubert, T., Rycroft, M., Farges, T., Blanc, E., Chanrion, O., Arnone, E., Odzimek, A., Arnold, N., Enell, C.F., Turunen, E., Bösinger, T., 2008. Recent results from studies of electric discharges in the mesosphere. Surv. Geophys. 29 (2), 71–137.
Pasko, V.P., Inan, U.S., Bell, T.F., Taranenko, Y.N., 1997. Sprites produced by quasi-electrostatic heating and ionization in the lower ionosphere. J. Geophys. Res. Space Physics 102 (A3), 4529–4561.
Pérez-Invernón, F.J., Gordillo-Vázquez, F.J., Luque, A., 2016. On the electrostatic field created at ground level by a halo. Geophys. Res. Lett. 43 (13), 7215–7222.
Pizzuti, A., Bennett, A., Fullekrug, M., 2019a. Using a short-range quasi-electrostatic thunderstorm detector for lightning safety and research. Geophysical Research Abstracts 21.

Pizzuti, A., Soula, S., Mlynarczyk, J., Bennett, A., Fullekrug, M., Pedeboy, S., 2019b. Signatures of Remote Intense Lightning on a Quasi-static Displacement Current Sensor. AGUFM (pp.AE21B-3070).
Pizzuti, A., Soula, S., Mlynarczyk, J., Bennett, A., Fullekrug, M., 2020, May. Analysis of sprite events during small-scale winter thunderstorms in northern Europe. In: EGU General Assembly Conference Abstracts, p. 20065.
Santolík, O., Kolmašová, I., 2017. Unusual electromagnetic signatures of european North Atlantic winter thunderstorms. Sci. Rep. 7 (1), 1–9.
São Sabbas, F.T., Sentman, D.D., 2003. Dynamical relationship of infrared cloudtop temperatures with occurrence rates of cloud-to-ground lightning and sprites. Geophys. Res. Lett. 30 (5).
São Sabbas, F.T., Sentman, D.D., Wescott, E.M., Pinto Jr., O., Mendes Jr., O., Taylor, M. J., 2003. Statistical analysis of space–time relationships between sprites and lightning. J. Atmos. Sol. Terr. Phys. 65 (5), 525–535.
Schulz, W., Diendorfer, G., Pedeboy, S., Poelman, D.R., 2016. The European lightning location system EUCLID–Part 1: Performance analysis and validation. Nat. Hazards Earth Syst. Sci. 16 (2), 595–605.
Scovell, R., Al-Sakka, H., 2016. A point cloud method for retrieval of high-resolution 3D gridded reflectivity from weather radar networks for air traffic management. J. Atmos. Ocean. Technol. 33 (3), 461–479.
Siingh, D., Singh, R.P., Singh, A.K., Kumar, S., Kulkarni, M.N., Singh, A.K., 2012. Discharges in the stratosphere and mesosphere. Space Sci. Rev. 169 (1–4), 73–121.
Sonnenfeld, R.G., Hager, W.W., 2013. Electric field reversal in sprite electric field signature. Mon. Weather Rev. 141 (5), 1731–1735.
Soula, S., Mlynarczyk, J., Pizzuti, A., Pedeboy, S., Gonneau, E., Gomez Kuri, Z., van der Velde, O., Montanya, J., Farges, T., Fullekrug, M., Bennet, A., 2020, May. Analysis of the lightning flashes associated with very large and luminous sprites in Western Europe. In: EGU General Assembly Conference Abstracts, p. 22263.
Wescott, E.M., et al., 2001. Triangulation of sprites, associated halos and their possible relation to causative lightning and micrometeors. J. Geophys. Res. https://doi.org/10.1029/2000JA000182.
Williams, E.R., 1998. The positive charge reservoir for sprite-producing lightning. J. Atmos. Sol. Terr. Phys. 60 (7–9), 689–692.